Protein J (2009) 28:161–168
DOI 10.1007/s10930-009-9179-y

A Novel Calcium Oxalate Crystal Growth Inhibitory Protein from the Seeds of *Dolichos biflorus* (L.)

Rakesh K. Bijarnia · Tanzeer Kaur · Surinder K. Singla · Chanderdeep Tandon

Published online: 2 June 2009

Abstract Recurrence and persistent side effects of present day treatment for urolithiasis restrict their use, so an alternate, using phytotherapy is being sought. *Dolichos biflorus* seeds, which are used as dietary food in India, possess antilithiatic properties. In the present study, a novel dimeric antilithiatic protein (98 kDa) from its seeds was purified based on its ability to inhibit calcium oxalate crystallization in vitro. Amino acid analysis of *Dolichos biflorus* antilithiatic protein showed abundant acidic amino acids. The mascot search engine presented sequence similarity with a calcium binding protein, calnexin of *Pisum sativum* from the m/z data obtained by MALDI TOF mass spectrometer. Above results demonstrate the anticalcifying/antilithiatic nature of a novel protein from the seeds of *Dolichos biflorus* and thus open new vistas for using plant proteins as therapeutic agents to treat urolithiasis.

Keywords *Dolichos biflorus* · Calnexin · Anticalcifying protein · Urolithiasis

Abbreviations

CNX	Calnexin
DAP	*Dolichos biflorus* antilithiatic protein
CaOx	Calcium oxalate
CO	Calcium oxalate monohydrate
C	Calcium oxalate dihydrate
FT	Fourier transform infrared spectroscopy
MALDI TOF	Matrix-assisted laser desorption/ ionization-time-of-flight mass spectrometry
RP	Reverse phase
HPLC	High pressure liquid chromatography
TFA	Trifluoroacetic acid
EG	Ethylene glycol
PMSF	Phenylmethane sulphonyl fluoride

R. K. Bijarnia · T. Kaur · C. Tandon (✉)
Department of Biotechnology and Bioinformatics,
Jaypee University of Information Technology, Waknaghat,
Solan 173215, India
e-mail: chanderdeep.tandon@juit.ac.in

R. K. Bijarnia
e-mail: rkchaudhary81@gmail.com

S. K. Singla
Department of Biochemistry, Panjab University,
Chandigarh, India

1 Introduction

Urolithiasis, one of the most painful ailment of the urinary tract, has beset humans from centuries. The formation of such concretion encompasses several physico-chemical events beginning with crystal nucleation, growth, aggregation [26] and ending by retention on renal tubular epithelial surfaces [27]. The mechanisms governing the induction of all these processes remain speculative. Calcium oxalate (CaOx) is the primary constituent of the majority of stones formed in the urinary system of patients with urolithiasis. Calcium oxalate monohydrate (COM), the thermodynamically most stable form, is observed more frequently in clinical stones than calcium oxalate dihydrate (COD) and it has greater affinity for renal tubular cells, thus responsible for the formation of stones in kidney [39]. In addition to CaOx, another form of calcium deposits, calcium phosphate precipitates, are common in individuals who are older than 35 year and are considered as relatively benign form of renal calcification [44]. One form of calcium phosphate stone i.e., brushite ($CaHPO_4$)

represents an early phase of calcium phosphate stone formation [11]. A nidus of brushite can elicit heterogeneous nucleation or epitaxial growth of calcium oxalate. Thus brushite has been implicated in the formation of both hydroxyapatite and CaOx stones [34]. The saturation state of body fluids with respect to stone-forming constituents and the presence of various biomolecules (inhibitors/stimulators) in the body fluids as well as organic matrix are known to influence mineralization [41, 2, 3, 29]. Certain stone inhibitory biomolecules such as proteins, lipids, glycosaminoglycans and inorganic compounds have been reported [37]. These kidney stone inhibitory biomolecules may keep the crystals from aggregating or accumulating as additional layers and thus prevent their growth.

Developments of modern techniques have revolutionized surgical management of the problem. Extracorporeal shock wave lithotripsy (ESWL) is currently the first-line treatment for upper urinary tract calculi. This treatment is not without side effects [42], and kidney damage during ESWL is a clinically significant problem [24]. The mechanisms underlying shockwave-induced renal tubular injury are not completely understood, though shear forces, thermal and cavitation effects, and free radical formation have been postulated [30, 40]. Therefore, it is worthwhile to look for an alternative for the management of urolithiasis. Many medicinal plants have been employed during ages to treat urinary stones though the rationale behind their use is not well established through systematic and pharmacological studies, except for some composite herbal drugs and plants [5, 18]. Interestingly, the areas having high consumption of these plant products, reported a very low incidence of urolithiasis and dietary patterns have been thought to play an important role for varied incidence of urinary calculi in the specific regions [14].

Dolichos biflorus is a leguminous pulse crop of subtropics. Its immature seeds are widely consumed as food in south Asian countries including rural areas of India. It is also used in folklore to treat urolithiasis [31]. So far, a few investigators have studied its efficacy on calcium mineralization. More recently, the seeds of *D. biflorus* were tested and compared with Cystone® (commercial drug) for their in vitro antilithiatic activity on calcium phosphate precipitation [12]. The extract of *D. biflorus* showed inhibitory activity almost equivalent to Cystone® towards calcium phosphate precipitation. Similar in vitro study showed the possibility of more than one biomolecules in *D. biflorus*, possessing the ability to inhibit calcium phosphate precipitation [35]. The present study aimed at examining the efficacy of *D. biflorus* and identification of the most potent biomolecule responsible for its antilithiatic property.

2 Materials and Methods

2.1 Materials

The seeds of *D. biflorus* were identified and then authenticated by microscopical and physiochemical data. The seeds were dried, powdered and stored before extraction. Other materials required were Macro Prep® 25 Q Strong anion exchanger (Bio-Rad laboratories), Bio gel® P-100 gel (Medium 90–180 μm) Molecular sieve support (Bio-Rad laboratories), carbonic anhydrase, alcohol dehydrogenase, bovine serum albumin, Trypsin profile IGD kit (Sigma, St. Lois, USA), Solvents used were of HPLC grade. All other chemicals were of analytical grade.

2.2 Crystal Growth Inhibition

Inhibitory activity against CaOx crystal growth was measured using the seeded, solution-depletion assay described previously [7, 32]. COM crystal seeds (from FTIR identified clinical kidney stones) were added to a solution containing 1 mM calcium chloride ($CaCl_2$) and 1 mM sodium oxalate ($Na_2C_2O_4$). The reaction of $CaCl_2$ and $Na_2C_2O_4$ with crystal seed would lead to deposition of CaOx on the crystal surfaces, thereby decreasing free oxalate that is detectable at λ214 nm. When a protein is added into this solution, depletion of free oxalate ions will decrease if the protein inhibits CaOx crystal growth. Rate of reduction of free oxalate was calculated using the baseline value and the value after 30-s incubation with or without protein. The relative inhibitory activity was calculated as follows: % Relative inhibitory activity $= [(C - S)/C] \times 100$, where C is the rate of reduction of free oxalate without any protein and S is the rate of reduction of free oxalate with a test protein.

Homogenous mineralization system was used to study the extent of in vitro mineral phase formation in the absence of any matrix [41]. This in vitro homogeneous assay system was modified by replacing 17.5 mM barbital buffer with 0.1 M Tris buffer (pH 7.4). The homogenous system consisted of 5 mM $CaCl_2$ and 5 mM KH_2PO_4. After incubating this system at 37 °C, precipitates obtained were centrifuged and the pellets were resuspended in 0.1 N HCl. The calcium (Ca^{2+}) and phosphate ions (HPO_4^{2-}) concentration in the precipitate represented the extent of precipitation (crystallization) of these ions and the inhibitory biomolecule(s) will minimize the extent of their precipitation. The $Ca^{2+}$and HPO_4^{2-} ions were estimated by the methods of Trinder [43] and Gomori [13], respectively. Percentage inhibition of mineral phase in the presence of test protein was calculated as: %age Inhibition $= [(C - T)/C] \times 100$, where T is the concentration of Ca^{2+}or HPO_4^{2-} ion of the precipitate formed in the assay system with the test protein and C is the

concentration of Ca^{2+}or HPO_4^{2-} ion of the precipitate formed in control system which had distilled water (Millipore).

2.3 Protein Purification

Powdered *D. biflorous* was extracted with 50 mM Tris–Cl buffer (pH 7.4), containing 0.25 M NaCl, 1 mM PMSF and 0.01% sodium azide for 24 h with gentle stirring at 4 °C. The slurry was centrifuged at 10,000*g* for 20 min at 4 °C to recover the supernatant. Protein in the supernatant was precipitated with ammonium sulfate (0–75% saturation) to recover the pellet with CaOx inhibitory activity. The pellet was dissolved in 50 mM Tris–Cl buffer containing 50 mM NaCl (pH 7.4) and dialyzed against the same buffer before fractionation on strong anion exchanger Macro Prep® 25 Q column (50 × 1.5 cm) pre-equilibrated with 20 mM Tris buffer with 0.1 mM NaCl (pH 7.4) using Biologic LP system (Bio-Rad). The elution was carried out with same buffer using a linear gradient of 0.1–1.0 M NaCl at flow rate of 1 ml/min. The fractions having anti-lithiatic activity were pooled, dialyzed against 50 mM Tris–Cl containing 50 mM NaCl and further fractionated on a Bio gel® P-100 gel molecular sieve column (70 × 2.5 cm) equilibrated and eluted with the 20 mM Tris buffer (pH 7.4) at a flow rate of 25 ml/h. The active fractions were pooled and the homogeneity was evaluated by electrophoresis and reverse phase HPLC. The purified protein was stored at −20 °C for further analysis.

2.4 Electrophoresis

SDS/PAGE was carried out using 10% polyacrylamide gels [22]. Native PAGE was carried out using 10% gels without using SDS or 2-mercaptoethanol. The molarity of the electrophoresis buffer used for native gels was 50 mM Tris–Cl and 284 mM glycine. The gels were over-run for 15 min for native PAGE and stained with Coomassie Brilliant Blue R-250.

2.5 Homogeneity and Molecular Mass of Purified Protein by HPLC

Homogeneity was ascertained by RP-HPLC, using a Waters Spherisorb® C18 (5μ, 4.6 × 250 mm) column with solvent A (0.1% TFA in water) and solvent B (100% acetonitrile containing 0.1% TFA). Protein was injected at a flow rate of 0.7 ml/min. The column was washed with solvent A for 5 min and brought to 50% acetonitrile in 7 min. The bound protein was eluted with a linear gradient of acetonitrile (50–70%) over a period of 60 min. The detection was monitored at 280 nm using Waters 2996 photodiode array detector.

The molecular mass of purified inhibitor protein was determined by gel filtration on HPLC using a Protein Pak 125 (300 × 7.8 mm) column, equilibrated with 20 mM sodium phosphate buffer (pH 7.2). The elution was carried out at a flow rate of 0.7 ml/min. The protein was detected at 280 nm using Waters 2996 photodiode array detector. The column was calibrated using standard proteins (carbonic anhydrase 29 kDa; Bovine serum albumin 68 kDa; alcohol dehydrogenase 150 kDa).

2.6 Amino Acid Analysis

Total amino acid content in the protein was estimated after acid hydrolyses of purified protein sample by the method of Elkin and Wasynczuk [10]. Derivatization of free amino acids after hydrolysis was performed by phenylisothiocyanate (PITC) and loaded on silica based column Pico Tag (Waters; 3.9 × 15 cm). Elution was done under high pressure using a gradient of sodium acetate trihydrate in 6% acetonitrile and 60% acetonitrile. The detection was done at a wavelength of 254 nm.

2.7 Isoelectric Point Determination

Isoelectric point was determined by the method of Yang and Langer [46]. Fully hydrated (20% v/v ethanol) Macro Prep® 25 Q Strong cation exchanger supports were utilized for determination of isoelectric point. After washing of matrix, it was equilibrated with 40 mM phosphate buffer of varying pH values. The purified protein, buffered with varying pH values corresponding to those of previously prepared resins were mixed and incubated (room temp, for 10 min) with the corresponding matrix. The supernatant was removed by centrifugation at 2,500*g* for 5 min and assayed at 280 nm for the presence of protein at all pH range. A graph was plotted between pH versus absorbance and isoelectric point was calculated using following equation. $pI = 1/m[\{(Y_H + Y_L)/2\} - b]$, where Y_H and Y_L are the absorbance values of higher and lower plateau of the Absorbance-pH plot respectively; m and b are constant and computed by straight line equation ($Y = mX + b$).

2.8 Peptide Mass Fingerprinting

The protein band was excised and subjected to in-gel tryptic digestion as using Trypsin profile IGD kit (Sigma). The resulting peptide mixtures were, eluted on the sample plate with the matrix solution (10 mg/ml of α-cyano-carboxycinnamic acid in 50% acetonitrile/0.1% trifluoro-acetic acid) and then analyzed on Bruker Ultraflex MALDI–TOF/TOF mass spectrometer. Peptide matching was performed using the MASCOT search engine (http://www.matrixscience.com) assuming that peptides were

monoisotopic, carbamidomethylated at cysteine residues, and oxidized at methionine residues. A mass tolerance was 1.2 Da, and only 1 maximal cleavage was allowed for peptide matching.

3 Results

The maximum inhibitory activity was recovered in the fraction precipitating at 75% ammonium sulfate saturation. The pellet obtained after 75% ammonium sulfate precipitation was desalted by dialysis and loaded on to anion exchanger. All fractions were collected and their protein content was determined [28]. The fractions which were obtained between conductivity 48.42 and 57.07 mS/cm (Fig. 1a), showed maximum inhibitory activity (81%). These fractions were pooled and further fractionated by molecular sieve chromatography on Bio gel (P-100 gel) column. Finally, a fraction (shaded in Fig. 1b) which eluted in a time span of 480–602 ml showing maximum inhibitory activity (92%) towards CaOx crystal growth was pooled and stored. The percentage yield and inhibitory activity of isolated fraction after each step is shown in Table 1.

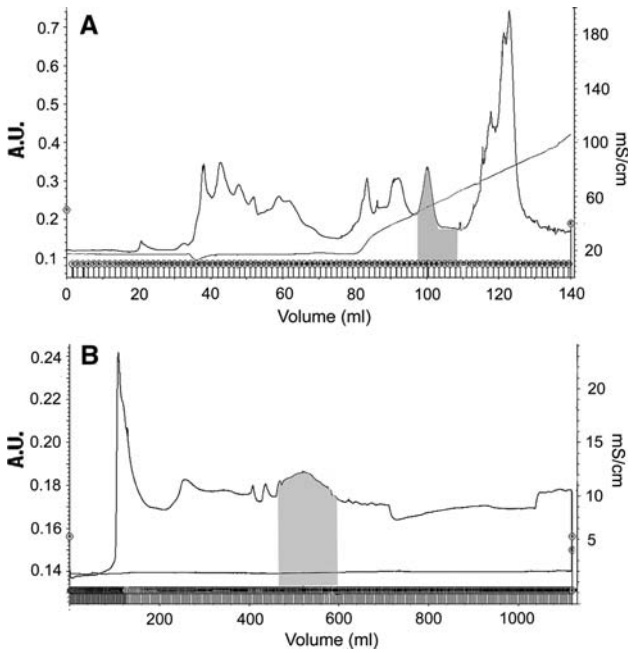

Fig. 1 Purification of active protein from *Dolichos biflorus*. **a** Elution profile of 96 mg of protein sample loaded on anion exchange chromatography column [Macro Prep® 25 Q column (50 × 1.5 cm)] after ammonium sulfate precipitation. The eluting proteins were detected at 280 nm. *Shaded portion* indicate elution of active fraction. **b** Elution profile of 16.5 mg protein loaded on molecular sieve column [Bio gel® P-100 gel (70 × 2.5 cm)] after anion exchange chromatography. The eluting proteins were detected at 280 nm. *Shaded portion* indicate elution of active fraction

3.1 Molecular Mass and Isoelectric Point Determination

SDS–PAGE analysis of the purified protein revealed two bands of molecular mass 58 and 34 kDa (Fig. 2a). Native PAGE showed single band (Fig. 2b) and homogeneity of the fraction was confirmed on RP-HPLC which revealed a single peak with a retention time of 21.4 min (Fig. 2c). The exact molecular mass of purified protein was determined by size exclusion HPLC. The molecular mass of purified protein was determined to be 98 kDa (Fig. 3a) on a standard curve plotted using protein markers in the range of molecular mass 29–150 kDa. The isolectric point of the purified protein was evaluated from the Fig. 3b. The slope (m) and Y-intercept (b) of straight line was calculated to be 0.5366 and −2.219 respectively, taking the values of higher and lower plateau from Fig. 3b, isoelectric point of protein was found to be 4.79.

3.2 Characterization of Inhibitory Activity of Purified Protein

Figure 4 shows the inhibitory activity of *D. biflorus* antilithiatic protein (DAP) at 50, 100 and 200 µg/ml. The data in Fig. 4a demonstrate the significant inhibition of crystal growth from 5 min of incubation to 1 h, till the end of the assay and there were significant differences among the three different concentrations of protein. It is evident from the Fig. 4 that with increase in concentration of protein its

Table 1 Summary of purification of inhibitory protein from the seeds of *Dolichos biflorus*

Purification steps	Total protein (mg)	Yield (%)	% Inhibition of CaOx by 1,000 µg/ml of protein sample
Tris buffer extract	137	100	65 ± 2.72
75% $(NH_4)SO_4$ Precipitate	96	70	73 ± 5.28
Anion exchange Chromatography	16.5	12	81 ± 3.11
Molecular Sieve chromatography	1.5	0.01	92 ± 3.73

% Age inhibition of CaOx represents results as mean ± SD ($n = 6$). Data refer to the protein obtained during various stages of purification from 30 g of powdered *Dolichos biflorus* seeds

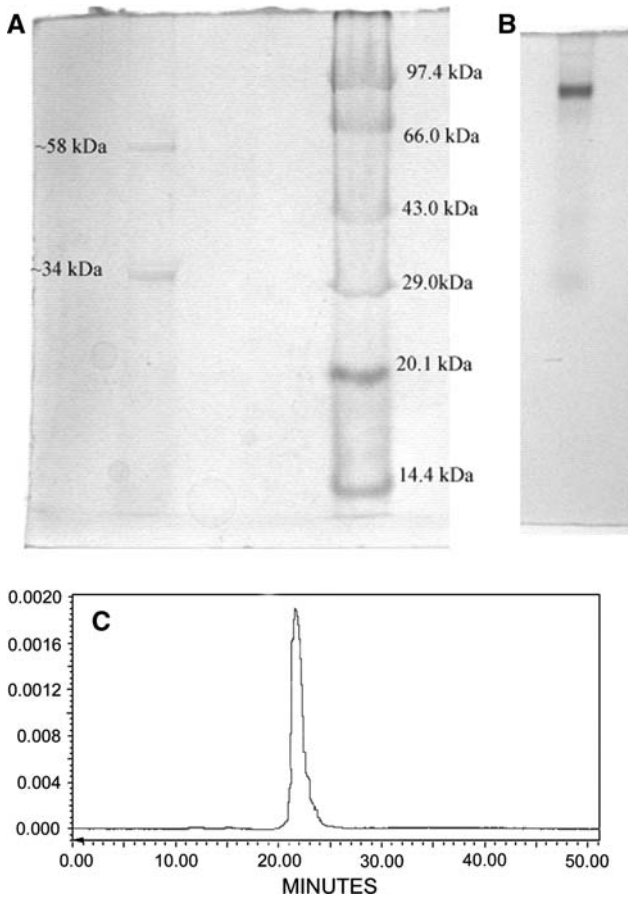

Fig. 2 **a** SDS–PAGE (10%) of DAP showing *two bands* of molecular mass 58 and 34 kDa. **b** Native PAGE profile of DAP showing a *single band*. **c** RP-HPLC of DAP for homogeneity, showing a *single peak* at 21.4 min [Waters Spherisorb® C18 (5μ, 4.6 × 250 mm) maintained at room temperature]

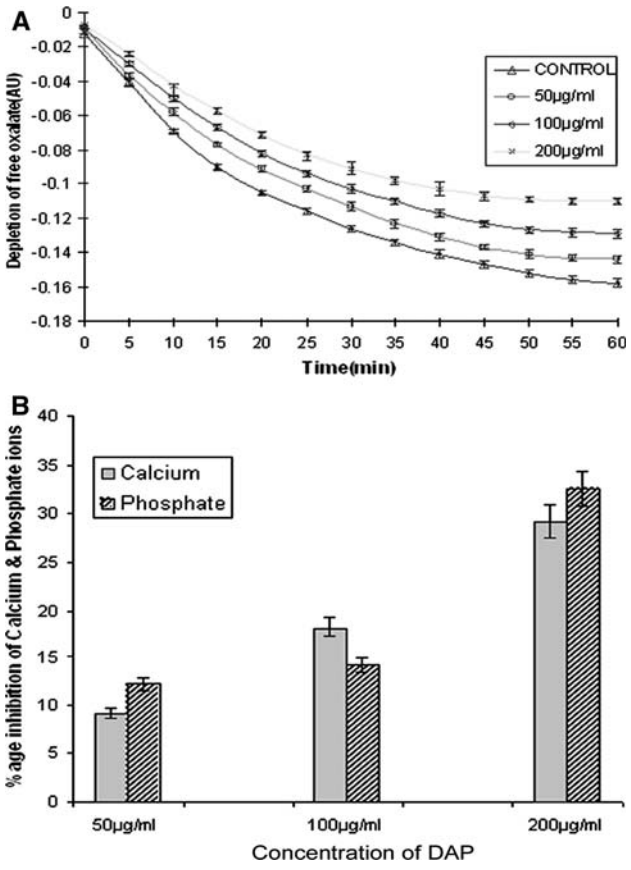

Fig. 4 **a** The kinetics of the CaOx crystal growth inhibitory activity by DAP at concentrations 50, 100 and 200 µg/ml as compared to control having Millipore water instead of DAP. The inhibitory activity was performed for a longer duration (60 min) to simulate the long term effects of interaction between crystals and DAP ($n = 6$). **b** Percentage inhibition of calcium and phosphate ions following calcium phosphate crystallization by DAP at concentration 50, 100 and 200 µg/ml ($n = 6$)

inhibitory activity also increased. On evaluating inhibitory potency of isolated protein on calcium phosphate crystallization, using similar concentrations of protein, again an increasing percentage inhibition of both calcium and phosphate crystallization was observed as shown in Fig. 4b.

3.3 Peptide Mass Fingerprinting of DAP and Amino Acid Analysis

MALDI TOF analysis spectrum of DAP is shown in Fig. 5. Using m/z ratio of all peptides obtained from mass

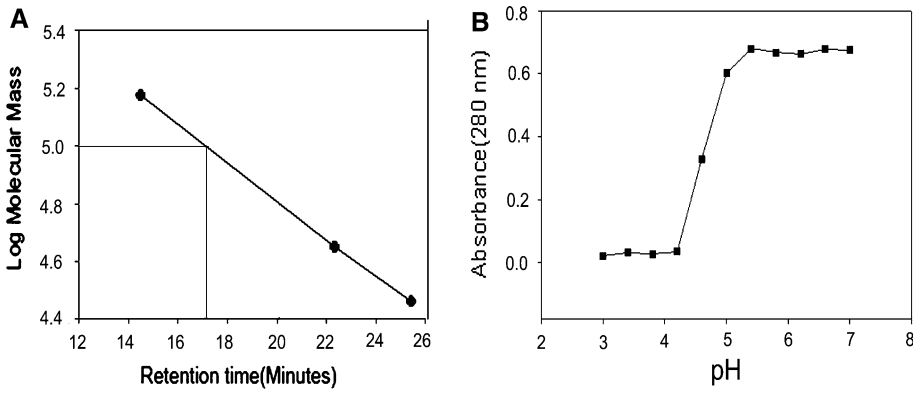

Fig. 3 **a** Determination of molecular mass of protein from *Dolichos biflorus* having CaOx inhibitory activity. Size exclusion HPLC of DAP and molecular-mass markers in the range 29–150 kDa. The *graph* represents standard curve and the mass of DAP is marked on the standard curve as 98 kDa. **b** Determination of Isoelectric point of DAP

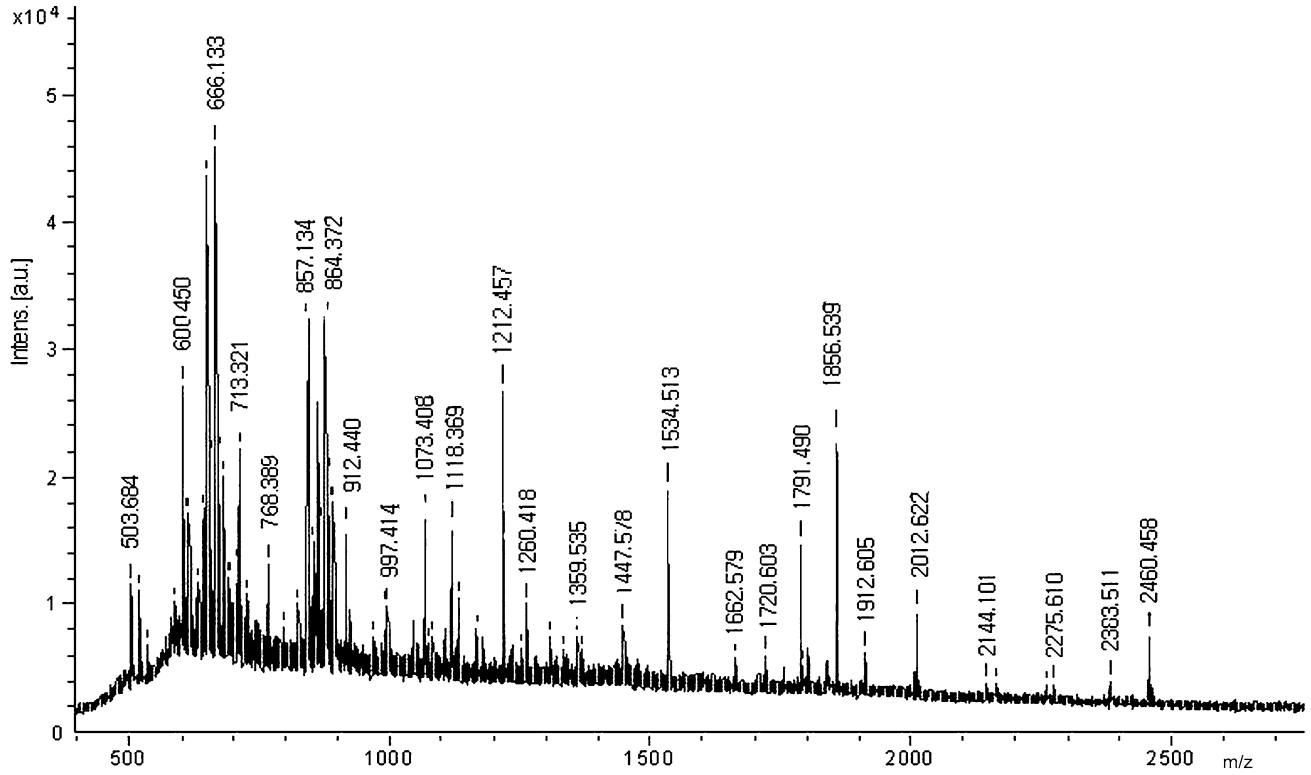

Fig. 5 The MALDI-TOF MS data obtained from DAP. Using MASCOT search engine, peptide masses from DAP showed 35% sequence similarity with calnexin protein and the identified residues obtained from MS data are *encircled*

spectrometer, the mascot search engine showed highest similarity (Score: 57) of DAP with calnexin (CNX) of *Pisum sativum* (CAA76741) having 35% sequence coverage. Amino acid analysis of the DAP showed that glutamate and aspartate are present in abundant amount (12.70 and 12.69%). In addition, relatively higher content of tyrosine and serine was also observed (Table 2).

4 Discussion

Due to significant side effects and failure to prevent recurrence by the present day treatment procedures of urolithiasis, alternative treatment modalities by herbal products have assumed importance. A dramatic advancement in using phytotherapy for urolithiasis treatments have been observed in recent years and many investigators have proposed to implicate scientific study on its efficacy [16]. Till date various plants extract have been studied to reduce the incidence of calcium stone deposition both in vivo and in vitro [4, 6, 19] but the identification of naturally occurring CaOx inhibitory biomolecules from plants was hampered in past by limitation in identification method.

Table 2 Amino acid composition of *Dolichos biflorus* antilithiatic protein (DAP)

Amino acids	Percentage of amino acid
Alanine (Ala)	2.49
Arginine (Arg)	0.63
Aspartic acid (Asp)[a]	12.69
Cysteine (Cys)	7.72
Glutamic acid (Glu)[b]	12.70
Glycine (Gly)	3.99
Histidine (His)	1.65
Isoleucine (Ile)	1.17
Leucine (Leu)	5.91
Lysine (Lys)	10.15
Methionine (Met)	3.15
Phenylalanine(Phe)	2.77
Proline (Pro)	1.62
Serine (Ser)	8.74
Threonine (Thr)	2.50
Tryptophan (Trp)	–
Tyrosine (Tyr)	7.82
Valine (Val)	3.97

[a] Include both aspartic acid and asparagines

[b] Include both glutamic acid and glutamine

Dolichos biflorus seeds are common dietary food of north India and are purported to have antilithiatic proficiency. There have been very few systematic studies on the antilithiatic properties of this plant [12, 21, 35]. The constituents of *D. biflorus* possessing antilithiatic property have not yet been identified.

Various CaOx crystal growth inhibitors mostly proteins and glycosaminoglycans have been reported in humans to play an important role in renal stone diseases for several decades [8, 47]. Most of these proteins have been isolated from CaOx kidney stones matrix itself in their active form [2, 3]. Likewise, many plants are also known to produce CaOx as crystalline deposits [33, 45], having an organic matrix constituting different proteins [25]. These proteins are believed to play an important role in the control of crystal growth and modification of crystal form [1]. More recently [17] four proteins from the organic matrix of CaOx crystals present in the seeds of *Phaseolus vulgaris*, have been isolated which inhibited the nucleation of CaOx crystallization in solutions. They have also shown that the isolated proteins modified the morphology of CaOx crystal mainly at {120} face (fastest growing face). A well known CaOx inhibitor, citrate, has also shown to slow the growth of {120} face [36]. Recently, our group has also purified an anticalcifying protein from the seeds of *Trachyspermum ammi* [20].

In the present study an antilithiatic protein was isolated from the seeds of *D. biflorus* inhibiting both calcium oxalate and calcium phosphate crystallization. The *D. biflorus* antilithiatic protein (DAP) (98 kDa, pI 4.79) showed two bands of molecular weight 58 and 34 kDa clearly indicates its dimeric nature. Previous studies claim that the non-protein part is responsible for the antilithiatic nature of *D. biflorus.* [12, 35]. The MALDI-TOF MS analysis of DAP showed maximum similarity (35% sequence coverage) with calnexin (CNX) protein of *P. sativum* (CAA76741). Although molecular weight of CNX (62 kDa) is not similar with DAP protein, but the pI of DAP is comparable with CNX. Since many plant databases are still largely incomplete, many proteins present in *D. biflorus* are absent in those databases. So protein DAP is not homologous with CNX, but probably is CNX like protein.

Calnexin, a type 1 membrane protein was found as an interacting protein in the biogenesis of class I histocompatibility molecules in ER [9]. A recently reported X-ray crystal structure shows that CNX consists of two domains, a globular domain and a long extended arm domain [38]. A lectin site was found within the concave surface of the globular domain and thus it makes its structural similarity to legume lectin family. Additionally, a calcium binding site was also identified within the globular domain [23]. On exploring the inhibitory potency of DAP on calcium phosphate crystallization again an effective inhibition was observed, thus clearly indicating that DAP is probably imparting its effect by binding to calcium ions. We proposed that DAP, which is CNX like protein has a calcium binding site, which might also be responsible for its ability to inhibit CaOx crystallization.

It has been suggested that acidic amino acid residues such as Asp and Glu, that are expected to be deprotonated and negatively charged at urinary pH, are attracted to positively charged calcium ions of COM [15]. Our data of amino acid analysis also suggests that DAP have higher acidic amino acids (Asp and Glu) content and similarly CNX also have high content of acidic amino acids (data not shown). Thus it could be argued that DAP, which is a CNX like protein possess the capability to inhibit calcium crystallization.

In conclusion, a plant protein from the seeds of *D. biflorus* was shown to attain the ability of inhibiting calcium oxalate crystallization in vitro. The protein was anionic in nature having abundant acidic amino acids and a similarity of this protein with calnexin of *P. sativum* was also found. Activity of this protein from *D. biflorus* adds a new vista to study plant proteins for their therapeutic use as antilithiatic proteins.

Acknowledgments The authors would like to thank Dr. S.·K. Singh, Department of Urology, Post Graduate Institute of Medical and Education research (PGIMER), Chandigarh, India for providing clinical calcium oxalate stones; Dr. Girish Sahni, Director, Institute of Microbial Technology (IMTECH), Chandigarh, India for amino acid analysis; Dr. P. Rama Rao, Director, National Institute of Pharmaceutical Education and research (NIPER), SAS Nagar, India for MALDI-TOF MS.

References

1. Addadi L, Weiner S (1985) Proc Natl Acad Sci USA 82:4110–4114
2. Aggarwal S, Tandon C, Forouzandeh M, Singla SK, Kiran R, Jethi RK (2000) Mol Cell Biochem 210:109–119
3. Aggarwal S, Tandon C, Forouzandeh M, Singla SK, Kiran R, Jethi RK (2005) Ind J Biochem Biophy 42:113–117
4. Atmani F, Farell G, Lieske JC (2004) J Urol 172:1510–1514
5. Barros ME, Schor N, Boim MA (2003) Urol Res 30:374–379
6. Christina AJM, Ashok K, Packialakshmi M, Tobin GC, Preethi J, Murugesh N (2005) Methods Find Exp Clin Pharmacol 27:633–638
7. Chutipongtanate S, Nakagawa Y, Sritippayawan S, Pittayamateekul J, Parichatikanond P, Westley BR, May FE, Malasit P, Thongboonkerd V (2005) J Clin Invest 115:3613–3622
8. Coe FI, Parks JH, Nakagawa Y (1991) Semin Nephrol 11:98–109
9. Degen E, Williams DB (1991) J Cell Biol 112:1099–1115
10. Elkin RG, Wasynczuk AM (1987) Cereal Chem 64:226–229
11. Evan AP, Lingeman JE, Coe FL, Shao Y, Parks JH, Bledsoe SB, Phillips CL, Bonsib S, Worcester EM, Sommer AJ, Kim SC, Tinmouth WW, Grynpas M (2005) Kidney Int 67:576–591
12. Garimella TS, Jolly CI, Narayanan S (2001) Phytother Res 15:351–355
13. Gomori HD (1941) J Lab Clin Med 27:955–960

14. Grases F, Costa-Bauza A, Prieto RM (2006) Nutr J 5:23
15. Gul A, Peter R (2007) Urol Res 35:65–71
16. Gürocak S, Küpeli B (2006) J Urol 176:450–455
17. Jáuregui-Zúñiga D, Reyes-Grajeda JP, Moreno A (2005) Plant Sci 168:1163–1169
18. Jethi RK, Duggal B, Sahota RS, Gupta M, Sofat IB (1983) Indian J Med Res 78:422–425
19. Joshi VS, Parekh BB, Joshi MJ, Vaidya AD (2005) Urol Res 33:80–86
20. Kaur T, Bijarnia RK, Singla SK, Tandon C (2009) Protein Pept Lett 16:173–181
21. Kumar P, Despande PS, Singh CM (1981) Bull Med Ethnobot Res 2:277–284
22. Laemmli UK (1970) Nature 227:680–685
23. Leach MR, Cohen-Doyle MF, Thomas DY, Williams DB (2002) J Biol Chem 277:29686–29697
24. Li X, He D, Zhang L, Xue Y, Cheng X, Luo Y (2007) Urol Res 35:193–199
25. Li X, Zhang D, Lynch-Holm VJ, Okita TW, Franceschi VR (2003) Plant Physiol 133:549–559
26. Lieske JC, Deganello S (1999) J Am Soc Nephrol 10:422–429
27. Lieske JC, Swift H, Martin T, Patterson B, Toback FG (1994) Proc Natl Acad Sci USA 91:6987–6991
28. Lowry OH, Rosbrough NJ, Farr AL, Randall RJ (1952) J Biol Chem 193:265–275
29. Moghadam MF, Tandon C, Aggarwal S, Singla SK, Singh SK, Sharma SK, Varshney GC, Jethi RK (2003) J Cell Biochem 90:1261–1275
30. Moran ME, Hynynen K, Bottaccini MR, Drach GW (1990) J Urol 142:388
31. Mukherjee T, Bhalla N, Singh G, Aulakh K, Jain HC (1984) Indian Drugs 21:224–228
32. Nakagawa Y, Kaiser ET, Coe FL (1978) Biochem Biophys Res Commun 84:1038–1044
33. Nakata PA (2003) Plant Sci 164:901–909
34. Pak CY, Poindexter JR, Peterson RD, Heller HJ (2004) J Urol 171:1046–1049
35. Peshin A, Singla SK (1994) Indian J Exp Biol 32:889–891
36. Qiu SR, Wierzbicki A, Orme CA, Cody AM, Hoyer JR, Nancollas GH, Zepeda S, De Yoreo JJ (2004) Proc Natl Acad Sci USA 101:1811–1815
37. Ryall RL (1996) Pediatr Nephrol 10:656–666
38. Schrag JD, Bergeron JJ, Li Y, Borisova S, Hahn M, Thomas DY, Cygler M (2001) Mol Cell 8:633–644
39. Schroder FH (1995) Kidney Int 48:129–138
40. Suhr D, Brummer F, Hulser DF (1991) Ultrasound Med Biol 17:761–768
41. Tandon C, Aggarwal S, Forouzandeh M, Jethi RK (1998) J Cell Biochem 68:287–297
42. Terlecki RP, Triest JA (2007) Urology 70:898–899
43. Trinder P (1960) Analyst 85:889–894
44. Verkoelen CF (2006) J Am Soc Nephrol 17:1673–1687
45. Webb MA (1999) Plant Cell 11:751–761
46. Yang VC, Langer R (1985) Anal Biochem 147:148–155
47. Zerwekh JE, Holt K, Pak CY (1983) Kidney Int 23:838–841